Phase Transformations in Bulk Nanostructured Potassium Niobiosilicate Glasses

P. Bergese,* I. Alessandri,† E. Bontempi, and L. E. Depero

INSTM and Chemistry for Technologies Laboratory, University of Brescia, via Branze, 38, 25123, Brescia, Italy

A. Aronne, E. Fanelli, and P. Pernice

Department of Materials and Production Engineering, INSTM and University of Naples Federico II, Piazzale Tecchio, 80125, Napoli, Italy

T. Boffa Ballaran and N. Miyajima

Bayerisches Geoinstitut, Universitaet Bayreuth, 95440, Bayreuth, Germany

V. N. Sigaev

Mendeleev University of Chemical Technology of Russia, Miusskaya sq. 9, 125190 Moscow, Russian Federation

Received: July 7, 2006; In Final Form: October 23, 2006

In potassium niobiosilicate (KNS) glasses, nanostructuring can be driven and controlled by thermal treatments at the glass transition temperature and/or by modulation of the chemical composition. The tight relationship between nanostructure and nonlinear optical properties suggests these bulk nanomaterials as an appealing route to nanophotonics. The focus of this paper is placed on assessing the phase transformations which occur in these materials upon annealing at the glass transition temperature and subsequent heating. High-temperature resolved X-ray diffraction (HTXRD) and high-resolution transmission electron microscopy (HRTEM) experiments are integrated with previously published results for in-depth insight. It will be shown that nanostructuring evolves from nucleation of niobium-rich nanocrystals, which are up to 20 nm large, uniformly distributed in the matrix bulk, and metastable. Formation kinetics as well as phase transformation of the nanocrystals are determined by the glass composition. Depending on it, nanocrystal nucleation can be preceded or not by phase separation, and the nanocrystals' phase transition can be of first or second order.

Introduction

Second harmonic generation (SHG) in glasses and glass ceramics has opened new frontiers in optical material science.[1−3] In particular, bulk nanostructured glasses and transparent glass ceramics based on ferroelectric or other highly polarizable phases are revealed to be an appealing route to nanophotonics. Actually, the pure nonlinear single crystals employed in standard frequency converters are expensive and require careful adjustments, while by contrast, isotropic materials, like bulk nanostructured glasses, are cheap and require hardly any adjustment.[4]

In these materials nanostructuring takes place as a consequence of phase separation and can be driven and controlled by proper thermal treatments and/or variation of the composition. The approach has been successfully adopted to obtain photonic structures consisting of microspheres of a few micrometers containing lithium niobate crystals dispersed in a silica-rich glassy matrix.[5] Another example is the precipitation of copper chloride nanosized particles in a glassy matrix, which was simply achieved by using a phase-separated borosilicate glass.[6] More recently, amorphous nanostructuring (formation of nanosized inhomogeneities) on the scale of 5−20 nm in potassium niobium silicate (KNS) glasses was induced through heat treatments close to the system glass transition.[7] For these systems the relative maximum of SHG efficiency takes place at the initial stage of phase separation, then shading off with the inhomogeneities of growth. This unusual behavior set the basis of a novel interpretation of the SHG mechanism in glasses as due to a combination of third-order nonlinearity with a spatial modulation of linear polarizability.[7]

From these examples it clearly emerges that bulk nanostructuring and optical behavior are tightly intertwined. Nevertheless, further investigations are needed to gain deeper insight into the phenomenon. On one side, it is of fundamental interest, since it should show intriguing mechanisms of SHG due to local (nanoscale) atoms arrangement. On the other side, it is of technological impact, as it is compulsory to allow manufacturing of glasses and glass ceramics with tailored SHG.

Our research moves from the above depicted scene. We are studying the structural and microstructural features of KNS and potassium titanium phosphate (KTP) nanostructured glasses with promising nonlinear optical properties,[7−11] focusing on the growth/nucleation of the coherent domains/crystals in the matrix. We believe that a definitive knowledge of the nanostructuring intermediate and final steps is a key step for achieving a reliable interpretation of the nonlinear optical properties.

* Corresponding author: telephone +0039033715574; fax +390303-702448; e-mail paolo.bergese@ing.unibs.it.

† Present address: LATEMAR and Chemistry for Technologies Laboratory, University of Brescia, via Branze, 38, 25123, Brescia, Italy.

10.1021/jp064285z CCC: $33.50
Published on Web 12/21/2006

We extensively investigated the KNS glasses by differential thermal analysis (DTA), standard X-ray diffraction (XRD), and bidimensional micro X-ray diffraction (microXRD^2), Raman and Fourier transform infrared (FTIR) spectroscopies, scanning electron and atomic force microscopies (SEM and AFM), and small-angle neutron scattering (SANS). Puzzling over these data allowed us to shed some light on the bulk nanostructuring of the material. It consists of two partially overlapped processes: binodal phase separation and subsequent segregation of niobium-rich regions nanometric in size.[7,8,12,13] This interpretation agrees well with the macroscopic properties of the glass and with previous observations on similar systems.[14]

However, the picture is still incomplete. Does nanostructuring mean nucleation in the matrix of nanocrystals with a (nonidentified) crystalline structure or does it mean organization of atoms in shorter coherent domains that provide local structure seeds whose order fades out in the matrix, thus lacking crystalline periodicity? To answer this crucial question, we integrated previous investigations in two complementary ways. The first consisted of imaging the nanostructures by high-resolution transmission electron microscopy (HRTEM) and the second of tracking nanostructuring by in situ high-temperature resolved X-ray diffraction (HTXRD).

Materials and Methods

All the glasses were synthesized from reagent-grade KNO_3, Nb_2O_5, and SiO_2 and subsequent quenching according to the procedure described elsewhere.[15] The resulting glasses were transparent and free of inclusions and bubbles. Their amorphous structure was checked by XRD. As-quenched glasses of two molar compositions were prepared, namely, xK$_2$O·yNb$_2$O$_5$·(100 − x − y)SiO$_2$, with $x = 20$ and $y = 25$ or $x = 23$ and $y = 27$. Hereafter they will be referred as 20-25-55 and 23-27-50 glasses, respectively. These molar compositions were chosen as potentially representative of different nanostructuring behaviors. In order to follow the bulk nanostructuring kinetics, two series of samples (one for each composition) covering the intermediate nanostructuring steps were prepared. According to previous results,[8] nanostructuring was induced by isothermally annealing in air the as-quenched samples at their glass transition temperature, T_g; the intermediate annealing times were fixed at 2, 10, and 24 h. The samples intended for HRTEM imaging were ground in fine powders. The samples intended for HTXRD and DTA analysis were prepared in bulk slices of proper dimensions to fit the instrument sample holders.

DTA measurements were performed by a Netzsch high-temperature DSC 404 with an Al_2O_3 pan as reference. The bulk glass samples (about 50 mg) were scanned by use of a Pt pan in which they were fitted by adding powdered Al_2O_3. This adjustment also allowed for more efficient heat transfer between the pan and the sample. All DTA curves were recorded in air at a heating rate of 10 °C min^{-1}.

HTXRD measurements were performed on a Philips X'Pert PRO diffractometer ($\theta/2\theta$ Bragg−Brentano geometry) equipped with a variable temperature chamber with a temperature control of ±1 °C (Anton Paar HTK 1200). Co Kα radiation (λ = 1.790 Å), generated by a sealed X-ray tube (45 kV × 40 mA), and a real-time multiple strip detector (X'Celerator by Philips) were used for all the experiments. In the HTXRD experiments the as-quenched glasses were nanostructured in situ by isothermal annealing at T_g and the nanostructuring was tracked by $\theta/2\theta$ scans. The overall temperature program of the experiments consisted of (1) fast heating (50 °C min^{-1}) from ambient temperature up to a temperature 80 °C lower than T_g, (2) heating up to T_g at a heating rate of 10 °C min^{-1}, (3) isothermal annealing of 10 h at T_g, (4) heating up to 955 °C at a heating rate of 10 °C min^{-1}, and (5) cooling down to ambient temperature at a heating rate of −10 °C min^{-1}. During heating and cooling (steps 2, 4, and 5) the samples were scanned every 10 °C. During the isothermal annealing at T_g, the samples were scanned every 30 min. All the scans were collected in isothermal condition and 5 min after the target temperature was reached (in order to allow for temperature equilibration). The angular range of all the scans was $25° < 2\theta < 41°$, with step size and time of 0.05° deg and 1 s, respectively.

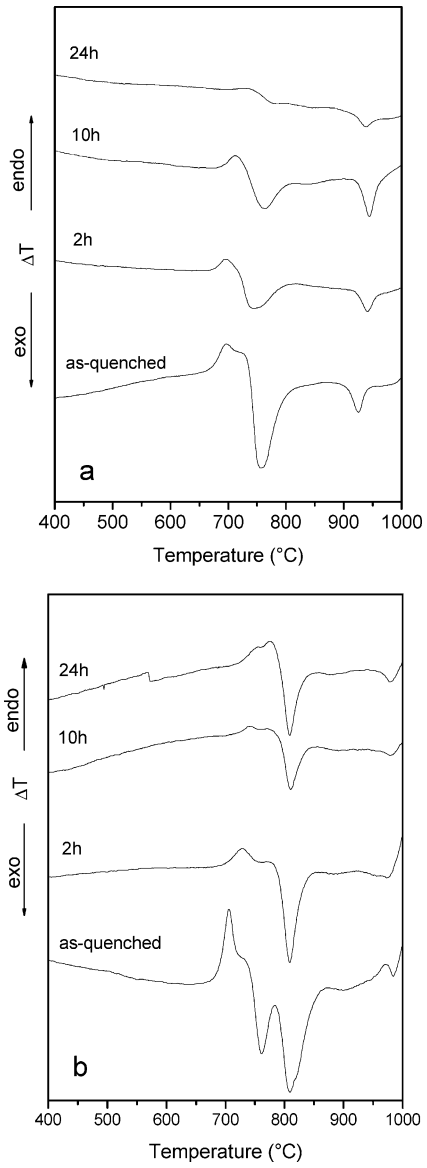

Figure 1. DTA curves of the sample series of composition 23-27-50 (a) and 20-25-55 (b).

HRTEM, selected area electron diffraction (SAED), and energy-dispersive X-ray spectroscopy (EDXS) were performed on a Philips CM20 FEG operating at 200 kV. The as-ground glass powders were imaged at the grain boundaries in transmission mode.

Results and Discussion

The DTA curves of the sample series of composition 23-27-50 and 20-25-55 are shown in Figure 1, panels a and b, respectively (the curves are shifted for clarity). The salient thermal data, obtained by analyzing the curves of the as-

TABLE 1: DTA Data for the 23-27-50 and 20-25-55 As-Quenched Glasses[a]

sample	T_g (°C)	T_1 (°C)	T_2 (°C)
23-27-50	680	757	925
20-25-55	705	760	810

[a] Glass transition temperature, T_g, and temperatures (modes) of the first, T_1, and the second, T_2, exothermic peak are shown.

quenched samples, are listed in Table 1. The glass transition temperature, T_g, was evaluated from the position of the inflection point at the slope change in the curves, and the temperatures of the first and the second exothermic peak, T_1 and T_2, are taken as the peak mode. The first and second exothermic peaks of the 20-25-55 as-quenched sample are closer, and partially overlapped, with respect to those of the 23-27-50 as-quenched sample. For both compositions the first peak is related to nanostructuring, while the second identifies a first-order phase transition, namely, the transition of the nanostructured phase into a crystalline phase, which differs from one composition to the other.[8] In the 23-27-50 series (Figure 1a) the intensity of the first peak shades with increasing annealing time, that is, as the nanostructuring process proceeds. The peak is absent in the DTA curve of the sample that was annealed for 24 h, suggesting that in that sample nanostructuring is complete. The 20-25-55 series (Figure 1b) shows an analogous, but faster, evolution of the first exothermic peak, as the peak is already absent in the DTA curve of the sample that was annealed for 2 h. These considerations suggest that the nanostructuring process in the two glasses follows different kinetics, that is, the nanostructuring kinetics is determined by the glass composition. According to previous observations,[7,8] we know that in the 23-27-50 glass nanostructuring occurs by binodal phase separation followed by segregation of niobium-rich regions nanometric in size. Instead, in the 20-25-55 glass nanostructuring may directly undergo the segregation route, skipping the step of phase separation. Faster relaxation kinetics may also explain why in the 20-25-55 glass the second exothermic peak, related to the nanostructured phase transformation, occurs at a lower temperature ($T_2 = 810$ °C) than in the 23-27-50 glass ($T_2 = 925$ °C).

HRTEM measurements were carried out for both the 23-27-50 and the 20-25-55 series, upon the as-quenched samples and the samples annealed at T_g for 2 and 24 h. Figure 2a,b shows two HRTEM micrographs resulting from the 23-27-50 and 20-25-55 as-quenched samples, respectively. As expected,[8] both samples are amorphous, since no planar fringes appear all over the investigated area. SAED patterns (representative ones are shown in the insets) confirm the morphological observation, exhibiting only the halos characteristic of the amorphous phase.

In Figure 3a,b the HRTEM micrographs of the samples annealed for 2 h are shown; insets show the SAED patterns. In both cases, clear-cut nanosized circular domains characterized by the coherent repetition of atomic planes (with a step of 0.5 nm) are detected. They indicate the presence of, probably, spherical nanocrystals dispersed into the amorphous matrix. In particular, in the case of the 20-25-55 sample (Figure 3b), there are several nanocrystals that are uniformly distributed all over the imaged area and have a size ranging from 7 to 15 nm. On the other hand, the 23-27-50 sample exhibits a lower number of smaller nanocrystals that give a weaker signal (5−7 nm, black circles in Figure 3a). The indications of the micrographs are confirmed by the SAED patterns, which show very different densities of the crystalline spots. All these observations, in agreement with the DTA results, hint that after 2 h of annealing the nanostructuring process is remarkably more advanced in the 20-25-55 sample.

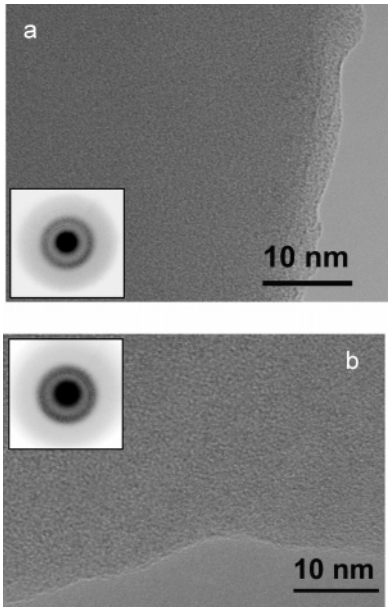

Figure 2. HRTEM micrographs of the as-quenched samples of compositions 23-27-50 (a) and 20-25-55 (b). (Insets) SAED patterns.

In both glasses the nanostructuring proceeds with annealing time, as witnessed by the HRTEM micrographs and the SAED patterns of the samples annealed for 24 h, which are shown in Figure 4. The nanocrystals are uniformly distributed, more numerous, and slightly bigger (from 10 to 20 nm for the 20-25-55 sample and less than 10 nm for the 23-27-50 sample) than the nanocrystals formed after 2 h of annealing. Thus, in both glasses nanostructuring evolves by nucleation of novel nanocrystals rather than by growth of the nanocrystals that nucleated during the early annealing hours. The nanocrystals of the 20-25-55 glass show more intense planar fringes and better-defined boundaries and look larger and more numerous, confirming the trend suggested by the 2 h annealed samples.

Two further conclusions can be drawn from the HRTEM experiments. First, for both glasses, at each annealing time, the EDXS data report a remarkable increase of the Nb/Si mass ratio in the nanocrystals with respect to the matrix (the integrated intensity ratios of the EDXS peaks related to Nb and Si are equal to 1.0 ± 0.1 and 1.7 ± 0.1 in the matrix and in the nanocrystals, respectively). This result confirms the hypothesis that nanostructuring is related to niobium segregation into nanometric regions.[7,8] Second, the nanocrystals grown in the two glasses of different compositions probably belong to the same crystallographic phase, as they show the same shape and interplanar distance in the HRTEM micrographs. This hypothesis could be directly confirmed by merging the electron diffraction profiles of the nanocrystals of the two glasses. Unfortunately, none of the SAED patterns collected for the 23-27-50 glass has enough statistics to extract a meaningful profile. However, DTA results support the hypothesis of a unique crystallographic phase. Actually, for both glasses the first exothermic peak, that HRTEM experiments confirm to be related to the nucleation of the nanocrystals, occurs at the same temperature (Figure 1 and Table 1).

Nanostructuring evolution upon heating was tracked on-line by HTXRD. The sequences of the HTXRD profiles for the 23-27-50 and 20-25-55 as-quenched glasses are showed in Figure 5, panels a and b, respectively (details about the heating programs are given in the Materials and Methods section). Each HTXRD experiment consisted of three steps: isothermal annealing at T_g for 10 h (gray-scale profiles in the figures), heating

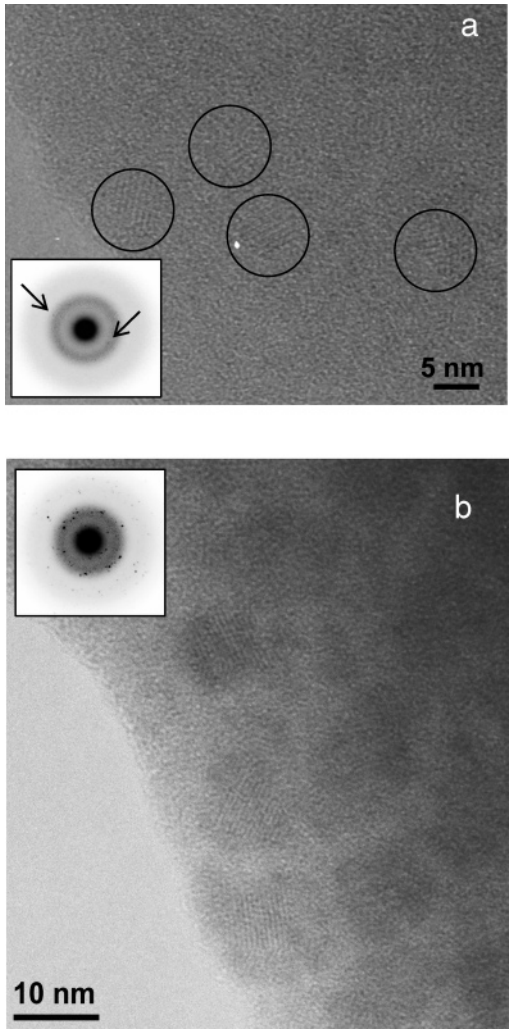

Figure 3. HRTEM micrographs of the samples of compositions 23-27-50 (a) and 20-25-55 (b) after 2 h of annealing. (Insets) SAED patterns. In panel a, some nanocrystals are highlighted by the black circles and in the inset some of the weak diffraction spots are indicated by the black arrows.

at 10 °C min^{-1} up to the phase transition of the nanocrystals, and cooling down at the same rate to ambient temperature. Comparison of the top profiles of Figure 5 panels a and b shows that the nanocrystals of both glasses transform into the same crystalline phase, which to date is unresolved. The Bragg peaks that appear only in the 20-25-55 top profiles belong to a crystalline silica phase. The new phase into which the nanocrystals transform was indexed on the basis of the recent papers by Narita et al.[16] and Enomoto et al.,[17] who determined the crystallographic structure of $K_{3.8}Nb_5Ge_3O_{20.4}$ phase. Results indicate that this phase, hereafter referred as NP, is probably characterized by an analogous stoichiometry, viz., $K_{3.8}Nb_5Si_3O_{20.4}$. Work is in progress to definitively define this aspect. The cooling sequences of the HTXRD profiles (see Supporting Information) evidence that the transition of the nanocrystalline phase into NP is not reversible on cooling, indicating that the nanocrystalline phase is metastable.

The appearance and growth of broad Bragg peaks in the profiles collected during isothermal annealing at T_g indicates the nanocrystals' nucleation. For both glasses the profile collected at the end of the annealing period has the main Bragg peak centered at $2\theta = 34.3°$. However, the diffraction profile of the 20-25-55 glass presents more and narrower peaks than that of the 23-27-50 glass. As suggested by HRTEM micrographs, this is probably due to the presence of more and larger nanocrystals. It is worthwhile to notice that the characteristics of these profiles (few and broadened Bragg peaks rising from a large amorphous halo) do not allow determination of the crystallographic phase of the nanocrystals.

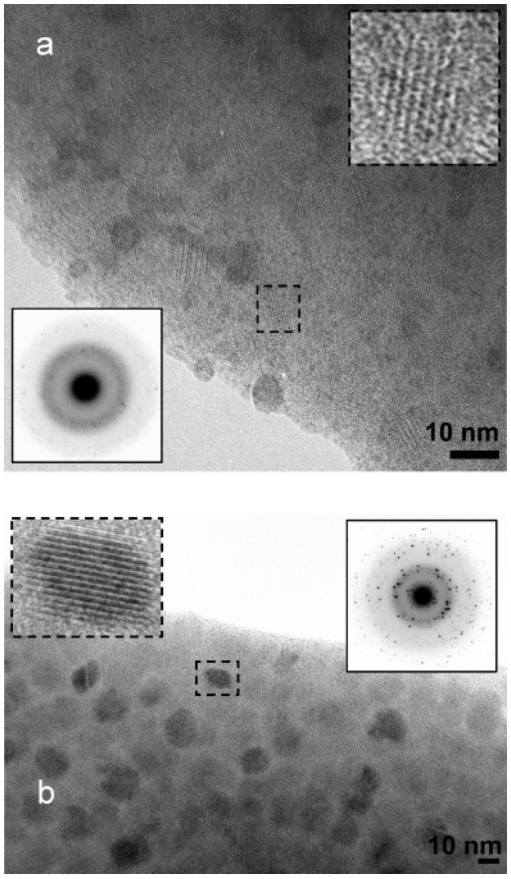

Figure 4. HRTEM micrographs of the samples of compositions 23-27-50 (a) and 20-25-55 (b) after 24 h of annealing. (Insets) SAED patterns and magnifications of the black dashed regions.

By analyzing the XRD profiles with the Debye−Scherrer method,[18] it results that after 10 h of annealing the average size of the nanocrystals is 3 and 10 nm for the 23-27-50 and the 20-25-55 glasses, respectively. This result, which refers to bulk macroscopic volumes, is fairly consistent with HRTEM observations. Actually, the size of the nanocrystals determined with Debye−Scherrer analysis (e.g., XRD) is lower than the size estimated from HRTEM imaging. This is due to the fact that the latter takes into account the nanocrystal boundaries, while the former probes only the coherent domains that constitute the nanocrystal cores.

The nanostructuring kinetics of the glasses can be drawn by plotting the normalized relative height of the most intense XRD peak ($2\theta = 34.3°$) versus the annealing time. These data, reported in Figure 6, confirm the indications given by DTA and HRTEM ex situ experiments: the 23-27-50 glass presents slower nanostructuring kinetics. Furthermore, since the curves do not reach a plateau, in neither glass is nanostructuring complete within 10 h of annealing.

The glasses of different compositions also display different behaviors upon heating. In the case of the 23-27-50 glass, the nanostructure attained during the annealing at T_g gradually "flows" with temperature into NP (Figure 5a). On the contrary, the 20-25-55 glass presents a stable nanostructure till 765 °C and then within a range of 20 °C undergoes a sudden transition (i.e., a discontinuous transformation) into NP (Figure 5b). These

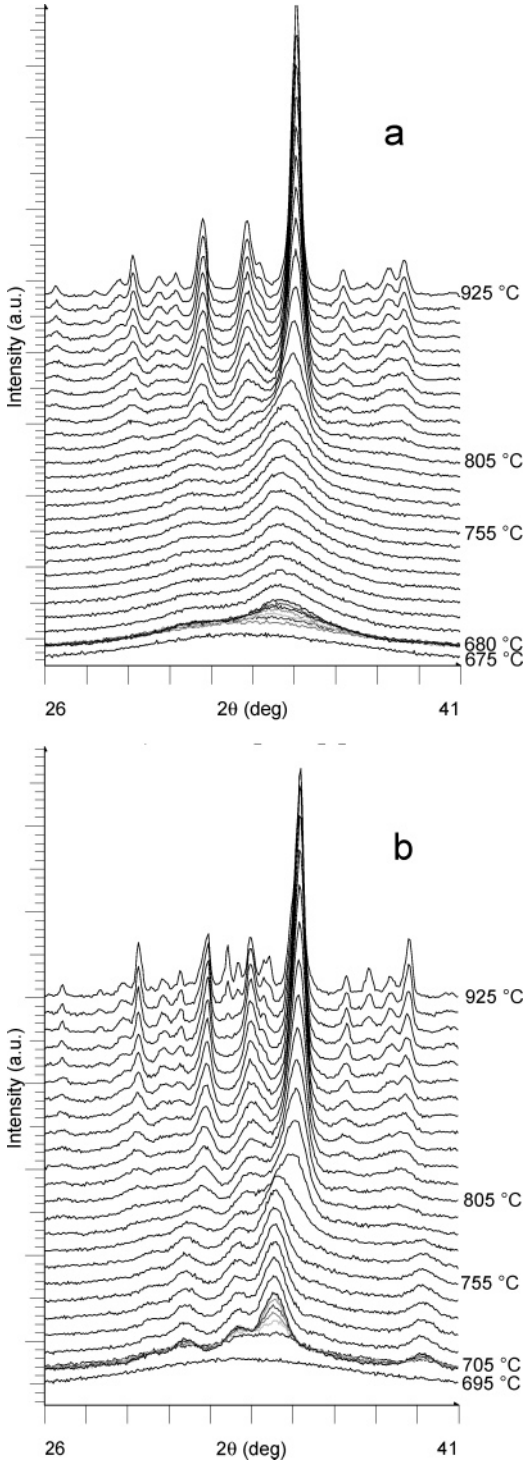

Figure 5. HTXRD profile series of 23-27-50 (a) and 20-25-55 (b) as-quenched glass. The samples were annealed in situ for 10 h at T_g; during annealing they were scanned each 0.5 h (gray-scale profiles; only the most representative are reported).

different behaviors can be also appreciated by considering Figure 7, where the temperature evolution of the full width at half-maximum (FWHM) of the most intense Bragg peak is shown (FWHM is inversely proportional to the size of the nanocrystals[18]). The curve trends confirm that the 23-27-50 glass is characterized by slower relaxation kinetics (continuous rearrangement of the amorphous matrix, which drives nucleation of niobium-rich nanocrystals).[8,12] In other words, the experimental evidence shown in Figures 5 and 7 suggest that the nanocrystals of the 23-27-50 composition transform into NP

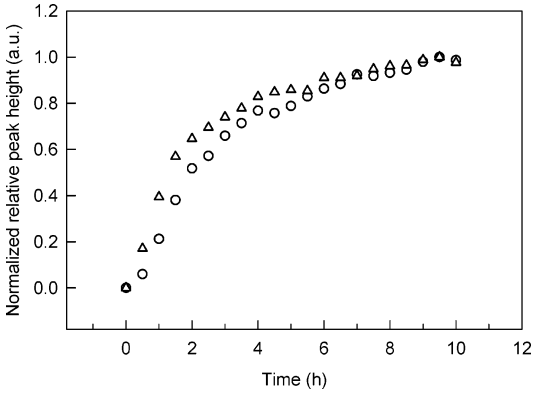

Figure 6. Nanostructuring kinetics of the 23-27-50 (○) and 20-25-55 (△) as quenched glasses during the in situ annealing at T_g (temperature-resolved XRD experiments). The kinetics (extent of reaction) are monitored by plotting the normalized relative height of the most intense XRD peak ($2\theta = 34.3°$) versus time (data obtained from the profiles reported in Figure 5).

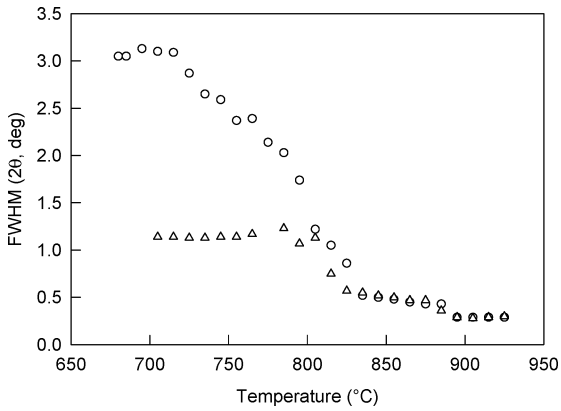

Figure 7. Temperature evolution of the fwhm of the most intense diffraction peak of the in situ 10 h annealed glasses 23-27-50 (○) and 20-25-55 (△). The data were obtained from the profiles reported in Figure 5.

by a continuous structural and microstructural change, that is, by a second-order (or kinetic) transformation. On the contrary, the nanocrystals of the 20-25-55 composition transform into NP by a discontinuous structural and microstructural change, that is, by a first-order (or thermodynamic) transformation.

For the 20-25-55 glass, the transition from DTA and HTXRD coincide. In contrast, for the 23-27-50 glass the transition determined by DTA is of first order at 925 °C, while the transition individuated by HTXRD is of second order and lies between 700 and 850 °C (Figure 7). This difference can be explained by considering that the heating runs of the HTXRD experiments were 30 times longer than the heating runs of the DTA experiments. Such amount of time slightly affects the phase transition of the nanostructured glass with faster kinetics. On the contrary, it allows the glass with slower kinetics to undergo another transition at lower temperatures.

Conclusions

We studied bulk nanostructuring in KNS glasses of two molar compositions, namely, $x\mathrm{K_2O}{\cdot}y\mathrm{Nb_2O_5}{\cdot}(100 - x - y)\mathrm{SiO_2}$, with $x = 20$ and $y = 25$ (20-25-55 glass) and $x = 23$ and $y = 27$ (23-27-50 glass).

In both glasses, nanostructuring, induced by isothermal annealing at the glass transition temperature, evolves from nucleation of novel nanocrystals rather than from growth of the nanocrystals nucleated during the early annealing stages. At the

end of 24 h of annealing in both glasses, the nanocrystals are uniformly dispersed in the matrix, but they are more numerous and slightly bigger in the 20-25-55 glass (from 10 to 20 nm in the 20-25-55 glass and less than 10 nm in the 23-27-50 glass). The nanocrystals of both glasses very likely belong to the same crystallographic phase, which is metastable.

The 23-27-50 glass presents slower and more complex nanostructuring kinetics. In particular, nanostructuring in the 23-27-50 glass occurs by rearrangement of the amorphous matrix, which then drives nucleation of niobium-rich nanocrystals. On the contrary, in the 20-25-55 glass nanostructuring probably turns directly into the nucleation route.

Upon slow heating, the nanocrystals of both glasses transform into the same (to date unresolved) crystalline phase. However, the nanocrystals belonging to the glasses of different compositions reach this new phase, NP, in a different fashion: in the 23-27-50 glass they undergo a second-order phase transition, while in the 20-25-55 glass they undergo a first-order phase transition.

Further investigations are in progress. They aim at identifying the crystallographic phase of NP, at interpreting the XRD data by the pair (radial) distribution function (PDF)[19] (which has been recently implemented for studying nanostructured and complex materials[20]), and at exploring the short-range order structure by X-ray absorption spectroscopy (XAS).

Acknowledgment. This research was founded by the Italian Ministry of Education, University and Research through the FIRB project RBNE0155X7 and COFIN 2004 project 200431757. HRTEM and HTXRD experiments were performed at the Bayerisches Geoinstitut under the EU "Research Infrastructures: Transnational Access" Programme [Contract 505320 (RITA) − High Pressure].

Supporting Information Available: Profile series relative to the cooling down HTXRD experiments. This material is available free of charge via the Internet at http://pubs.acs.org.

References and Notes

(1) Vogel, E. M.; Weber, M. J.; Krol, D. M. *Phys. Chem. Glasses* **1991**, *32*, 231.

(2) Nie, W. *Adv. Mater.* **1993**, *5*, 520.

(3) Nazabal, V.; Fargin, E.; Videau, J. J.; Le Flem, G.; Le Calvez, A.; Montant, S.; Freysz, E.; Ducasse, A.; Couzi, M. *J. Solid State Chem.* **1997**, *133*, 529.

(4) Skipetrov, S. E. *Nature* **2004**, *432*, 285.

(5) Lipovskii, A. A.; Petrikov, V. D.; Melehin, V. G.; Tagantsev, D. K.; Tatarintsev, B. V. *Solid State Commun.* **2001**, *117*, 733.

(6) Yoon, Y. K.; Han, W. T.; Chung, S. J. *J. Non-Cryst. Solids* **1996**, *203*, 195.

(7) Sigaev, V. N.; Stefanovich, S. Y.; Champagnon, B.; Gregora, I.; Pernice, P.; Aronne, A.; Le Parc, R.; Sarkisov, P. D.; Dewhurst, C. *J. Non-Cryst. Solids* **2002**, *306*, 238.

(8) Aronne, A.; Sigaev, V. N.; Pernice, P.; Fanelli, E.; Usmanova, L. Z. *J. Non-Cryst. Solids* **2004**, *337*, 121.

(9) Sigaev, V. N.; Fanelli, E.; Pernice, P.; Depero, L. E.; Sarkisov, P. D.; Aronne, A.; Bontempi, E.; Stefanovich, S. Y. *J. Non-Cryst. Solids* **2004**, *345*−*346*, 676.

(10) Sigaev, V. N.; Pernice, P.; Depero, L. E.; Aronne, A.; Bontempi, E.; Akimova, O. V.; Fanelli, E. *J. Eurp. Ceram. Soc.* **2004**, *24*, 1949.

(11) Aronne, A.; Depero, L. E.; Sigaev, V. N.; Pernice, P.; Bontempi, E.; Akimova, O. V.; Fanelli, E. *J. Non-Cryst. Solids* **2003**, *324*, 208.

(12) Aronne, A.; Sigaev, V. N.; Champagnon, B.; Fanelli, E.; Califano, V.; Usmanova, L. Z.; Pernice, P. *J. Non-Cryst. Solids* **2005**, *351*, 3610.

(13) Colombi, P.; Bergese, P.; Bontempi, E.; Pernice, P.; Aronne, A.; Sigaev, V. N.; Depero, L. E. *Proceedings of the 2nd National Conference on Nanoscience and Nanotechnology: The Molecular Approach*; Area del CNR di Bologna, 25−27 February 2004; p 199.

(14) Hart, R. T., Jr.; Anspach, M. A.; Kraft, B. J.; Zaleski, J. M.; Zwanziger, J. W.; DeSanto, P. J.; Stein, B.; Jacob, J.; Thiyagarajan, P. *Chem. Mater.* **2002**, *14*, 4422.

(15) Pernice, P.; Aronne, A.; Sigaev, V. N.; Sarkisov, P. D.; Stefanovich, S. Y.; Molev, V. I. *J. Am. Ceram. Soc.* **1999**, *82*, 3447.

(16) Narita, K.; Takahashi, Y.; Benino, Y.; Fujiwara, T.; Komatsu, T. *Opt. Mater*. **2004,** *25*, 393.

(17) Enomoto, I.; Benino, Y.; Fujiwara, T.; Komatsu, T. J. *Solid State Chem.* **2006**, *179*, 1821.

(18) Cullity, B. D. *Elements of X-ray diffraction*, Addison-Wesley: London, 1978; pp 99−106.

(19) Wright, A. C. *Glass Phys. Chem.* **1998**, *24*, 148.

(20) Egami, T.; Billinge, S. J. L. *Underneath the Bragg-Peaks: Structural Analysis of Complex Materials*; Plenum: Oxford, U.K., 2003.